ELSEVIER

Chemical Engineering Journal 142 (2008) 78–86

Chemical Engineering Journal

www.elsevier.com/locate/cej

Characterisation and comparison of the micromixing efficiency in torus and batch stirred reactors

L'hadi Nouri [a,*], Jack Legrand [b], Nabila Benmalek [a], Faiza Imerzoukene [a], Ahmed-Reda Yeddou [c], Farid Halet [c]

[a] *L.R T.A. FSI, Université M'hamed Bougara de Boumerdès, 35000 Boumerdès, Algeria*
[b] *GEPEA, Université de Nantes, CNRS, UMR 6144, CRTT-BP 406, 44602 Saint Nazaire Cedex, France*
[c] *L.E.D.T.E.G.E., Ecole Normale Supérieure de Kouba, Algeria*

Received 3 September 2007; received in revised form 15 January 2008; accepted 23 January 2008

Abstract

The mixing at a molecular scale (micromixing) plays an important role on selectivity, yield and quality of final products of a large range of competing fast chemical reactions. In this study, we have compared, by the use of iodide–iodate reaction tests, the micromixing in two reactors, the first one is the standard batch stirred reactor and the second is the torus reactor. Various conditions of agitation and feed locations were used for this study. A comparative analysis of the micromixedness ratio (α) in the two reactors was carried out on the basis of the local rate of specific energy dissipation.

Keywords: Micromixing; Segregation index; Reactors; Mixing efficiency

1. Introduction

Agitation is the mean by which the mixing of several miscible or not miscible phases can be achieved, and by which mass and heat transfer can be enhanced between phases or with the external surface wall of the reactor.

The study of the effect of mixing on the chemical or biological reactions is a very active field of research since the pioneer works of Danckwerts [1] and Zweitering [2]. Since, many experimental works and numerical computer codes have been developed, allowing to describe the mixing and the micromixing in the reactors.

The mixing process of the reactional fluid is naturally characterised by three scales, namely macromixing corresponding at the reactor or process scales, micromixing describes the mixing at a microscopic scale and mesomixing at the impeller scale. In many practical cases, a strong nonlinear coupling exists between reaction and transport phenomena at micro- and mesoscales and the reactor performance at the macroscale. A significant limitation of the phenomena of transport at a molecular scale can have an influence on the behaviour of the process and consequently on the reactor performance. Thus, the micromixing may influence selectivity, yield and quality of final products in many industrial processes, such as precipitation pharmaceutical products, polymerization, crystallization, consecutive reactions, parallel reactions, combustion, enzymatic catalytic reactions, etc. A slow mixing can delay desired reactions and promote undesired side reactions. For example, in the addition of an acid or base to a solution of an organic substrate, a slow mixing limits the neutralization reaction, which will allow the organic substrate to react with acid or base [3].

In the last decades, a lot of works has been done on micromixing, developing experimental methods to characterise it. Iris et al. [4] studied in semi-batch stirred reactors, the effect of the mixing on the quality product of a parallel reaction. They established a model predicting the product distribution of a competitive reaction for different hydrodynamic parameter. Aslund et al. [5] studied in a stirred tank reactor the effect of the agitation conditions and geometrical characteristics of the impeller on the reaction of precipitation of the benzoic acid. They noted that the size of the crystallized particles depends strongly on the intensity of agitation. Fang et al. [6] estimated qualitatively the segregation index in a continuous stirred tank reactor on the basis of parallel competing reaction, iodide–iodate. Although

* Corresponding author. Tel.: +213 70737273; fax: +213 24816333.
E-mail address: hnouri2001@yahoo.fr (L. Nouri).

1385-8947/$ – see front matter © 2008 Elsevier B.V. All rights reserved.
doi:10.1016/j.cej.2008.01.030

Nomenclature

d	impeller diameter (mm)
D	stirred batch reactor diameter (mm)
D_O	optical density
D_t	inner diameter of torus reactor (mm)
H	liquid height in stirred batch reactor (mm)
L	optical path length (mm)
LDV	laser Doppler velocimetry
L_t	total mean length of the torus reactor (mm)
N	stirring speed (rpm)
N_P	power number
P_i	feed location (i)
PIV	particle image velocimetry
PVC	poly-vinyl chloride
r	radial coordinates of feed location in stirred batch reactor (mm)
R	radius of the torus reactor (mm)
V	reaction volume (l)
X_s	segregation index
Y	ratio of sulphuric acid mole number consumed by reaction (2) divided by the total acid mole number injected
Y_{ST}	value of Y in total segregation case
z	axial coordinates of feed location in stirred batch reactor (mm)
Z_t	axial coordinate of feed location in the torus reactor by report the impeller (mm)

Greek letters

α	micromixedness ratio
$\bar{\varepsilon}$	mean rate of specific energy dissipation (W/kg)
ε	local rate of specific energy dissipation (W/kg)
ε_m	molar extinction coefficient (m^2/mol)
ϕ	proportionality constant

the feed rate in the reactor remained very low compared to the rate of recirculation, they noted that the mixing at a molecular scale (micromixing) is affected by the feed rate.

Several reactive mixing models were established, among them the coalescence–redispersion model [7], interaction by exchange with mean model [8], engulfment deformation–diffusion model [9], the engulfment model [10] and the two and three environment models [11,12]. Many works relating to modelling were undertaken, particularly by Baldyga and Bourne [13], Fournier [14], Guichardon [15] and Assirelli et al. [16] in order to estimate the various characteristics of the micromixing, such as, time of micromixing and local specific energy dissipation rate. On the other hand, other experimental techniques, like laser Doppler velocimetry (LDV) [17,18] and particle image velocimetry (PIV) [19], have significantly improved the determination values of local specific energy dissipation rate (ε), from which, local micromixing time (t_m) was determinate by using the Kolmogorov's theory.

Until now, the importance and the impact of this phenomenon at a molecular scale on the selectivity, the yield and the quality of the chemical or biological synthesis products attracted a very great number of researchers. Many types of reactors such as, stirred tank reactor [20,21], impinging jets reactor [22], static mixer [23,24], rotating packed bed [25,26], tubular reactor [27] and Couette flow reactor [28] have been studied at a micromixing point of view. On the other hand, many experimental data obtained with test reaction showed that physical parameters, such as feed location and impeller speed have an effect on the distribution of reaction product.

The aim of this study is firstly to characterise the micromixing efficiency in the torus and the batch stirred reactors by the use of reaction test, and secondly to compare the micromixing efficiency in both reactors on the basis of the local rate of specific energy dissipation.

2. Experimental

2.1. Description of the experimental device

The experiments were carried out in two reactors with different configurations. The first one is a stirred tank reactor of 1.871 nominal volume, equipped with a standard Rushton turbine and four baffles placed at 90° intervals (Fig. 1). The second one is a torus reactor, similar at those used by Belleville et al. [29] and Nouri [30], constructed from four poly-vinyl chloride (PVC) beds of inner diameter (D_t) of 55 mm. The total mean length of the torus reactor is 884 mm, which corresponds to a volume of 2.11 (Fig. 2). The mixing and the flow were achieved by a marine screw impeller, driven by a variable speed motor (Heidolph RZR 2021). The geometrical characteristics of both reactors are given in Tables 1 and 2.

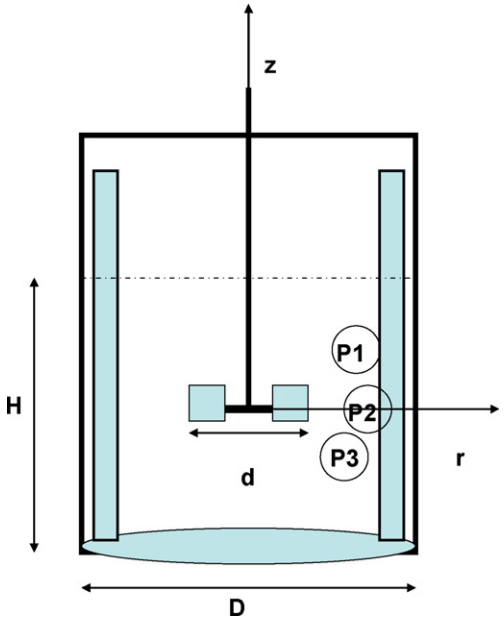

Fig. 1. Schematic of the batch stirred reactor used in this work.

Table 1
Geometrical characteristics of the batch stirred reactor and the impeller

V (l)	D (mm)	d (mm)	H (mm)	Coordinates of feed location in the batch stirred reactor by report the impeller					
				P1		P2		P3	
				z (mm)	r (mm)	z (mm)	r (mm)	z (mm)	r (mm)
1.87	133.5	64	133.5	32	47	0	47	−7	47

Table 2
Geometrical characteristics of the torus reactor and the impeller

d (mm)	V (l)	R (mm)	D_t (mm)	L_t (mm)	Coordinates of feed location in the torus reactor by report the impeller plane (Z_t)		
					P1	P2	P3
43.5	2.1	135	55	884	−100	−20	+20

2.2. Experimental method

2.2.1. The test reaction

There are several chemical methods used to determine micromixing of a fluid stream into a bulk mixture. The choice of a good test reaction should fulfill several conditions: simple reaction schemes in order to avoid analysis of many products; easy analysis of reaction products; known reaction kinetics, faster reaction rate than mixing rate; and good sensitivity and reproducibility [31].

Many authors have proposed consecutive and parallel competing reactions whereby the state of micromixing in the reactors can be characterised. Among the several chemical reactions tests proposed in the literature to characterise the micromixing, we have selected the well-known iodide–iodate method, proposed and developed by Villermaux et al. [31,32]. On the other hand, the iodide–iodate test offers the advantages of being cheap and easy to handle [33].

The chemical method adopted is based on competitive parallel reactions system. This reaction scheme consists in the following three chemical reactions:

$$H_2BO_3^- + H^+ \rightleftarrows H_3BO_3 \qquad \text{quasi-instantaneous} \qquad (1)$$

$$5I^- + IO_3^- + 6H^+ \rightleftarrows 3I_2 + 3H_2O \qquad \text{veryfast} \qquad (2)$$

$$I_2 + I^- \rightleftarrows I_3^- \qquad (3)$$

The neutralization reaction (1) is quasi-instantaneous, and redox reaction (2) (called Dushman reaction) is very fast, in the same range of the micromixing process.

For perfect micromixing conditions, the injected H^+ ions were instantaneously consumed by reaction (1) and reactions (2) and (3) may not occur. On the contrary, in imperfect mixing conditions, the injected H^+ ions were consumed competitively by reactions (1) and (2), and the iodine (I_2) formed can further react with iodide ions (I^-) to yield tri-iodide ions (I_3^-) according to the quasi-instantaneous equilibrium reaction (3). The amount of (I_3^-) produced, depends on the micromixing efficiency and allows quantifying the segregation intensity through a segregation index X_s.

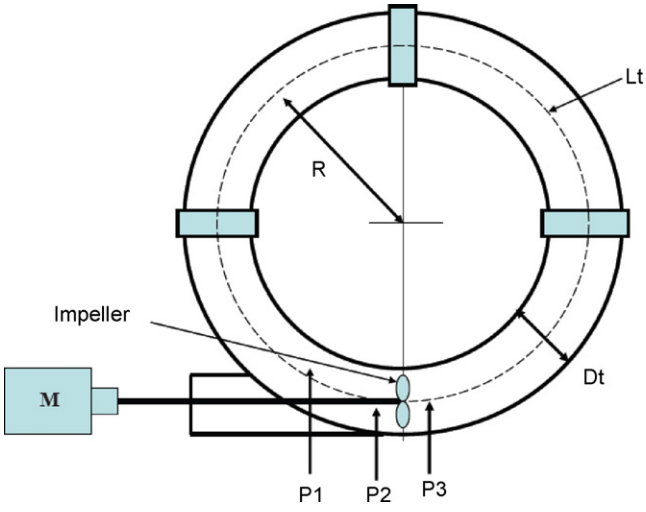

Fig. 2. Schematic of the torus reactor used in used in this work.

2.2.2. The procedure for preparation of solution

Initially, the boric acid solution (H_3BO_3) was added to sodium hydroxide solution (NaOH) to obtain an equimolecular buffer solution mixture $H_2BO^-{}_3/H_3BO_3$ (pH 9.14). Then, the concentrated solutions of potassium iodate and potassium iodide were introduced into the bulk and completed with water. The reactant concentrations used were chosen according to Guichardon and Falk [32] works and are summarised in Table 3.

Table 3
Reactant concentrations used

Reactants	Concentrations (M)
NaOH	0.0909
H_3BO_3	0.1818
KIO_3	2.33×10^{-3}
KI	1.17×10^{-2}

2.2.3. Experimental procedure

Two procedures can be applied to characterise micromixing in a reactor. The first procedure is based on the single injection, using a peristaltic pump, via a feed pipe of a small quantity about 1/1000 of the reaction volume of sulphuric acid (4 M) in the bulk containing iodide, iodate and borate ions. The flow rate of the sulphuric acid solution was determined by a preliminary study. Ten minutes after the end of acid injection, a sample of the solution was taken from the reactor, and the concentration of I_3^- ions was easily measured by spectrophotometry at 353 nm, such as

$$[I_3^-] = \frac{D_O}{\varepsilon_m \cdot L} \tag{4}$$

where L is the optical path length, equal to 1 cm, D_O is the optical density, ε_m is the molar extinction coefficient of I_3^- ions at 353 nm, equal to 2395.9 m^2/mol [34].

The second procedure is quasi similar to the previous one, but by using successive acid injections to characterise micromixing (one measure per each injection). Each injection corresponded to a small quantity of about 2/1000 of the reaction volume of sulphuric acid (1 M). This procedure developed by Guichardon and Falk [32] presents the advantage of micromixing characterisation for large vessels by reducing preparation time and experiments cost. In this study, we have adopted both procedures to compare them.

2.2.4. Determination of the segregation index X_S

The segregation index, X_s, is defined to quantify the micromixing quality, as the relative amount of sulphuric acid, which is consumed to yield iodine [31]. For the procedure corresponding to the simple injection, X_s is defined by

$$X_s = \frac{Y}{Y_{ST}} \tag{5}$$

where Y is the ratio of sulphuric acid mole number consumed by reaction (2) divided by the total acid mole number injected, Y_{ST} is the value of Y in total segregation case. X_s values vary between 0 and 1, such as $X_s = 0$, perfect micromixing; $X_s = 1$, total segregation; $0 < X_s < 1$, partial segregation, where

$$Y = \frac{2(n_{I_2} + n_{I_3^-})}{n_{H_O^+}} = \frac{2V_{reactor}([I_2] + [I_3^-])}{V_{injection}[H^+]_O} \tag{6}$$

$$Y_{ST} = \frac{6[IO_3^-]_O}{6[IO_3^-]_O + [H_2BO_3^-]_O} \tag{7}$$

The concentration of I_2 used in the Eq. (6) is obtained from Eq. (10), by combining equations of the mass balance on iodine ions yield (Eq. (8)) and the equilibrium constant K_B of reaction (3) (Eq. (9)).

$$[I^-] = [I^-]_O = -\frac{5}{3}([I_2] + [I_3^-]) - [I_3^-] \tag{8}$$

$$K_B = \frac{[I_3^-]}{[I_2][I^-]} \tag{9}$$

$$-\frac{5}{3}[I_2]^2 + \left([I^-]_O - \frac{8}{3}[I_3^-]\right)[I_2] - \frac{[I_3^-]}{K_B} = 0 \tag{10}$$

where K_B is the equilibrium constant of reaction (3), given by the following equation

$$\log_{10} K_B = \frac{555}{T} + 7.355 - 2.575 \log_{10} T \tag{11}$$

For the procedure corresponding to successive injections, X_{s_i} for each injection is defined by

$$X_{s_i} = \frac{Y_i}{Y_{ST,i}} \tag{12}$$

The index i corresponding to the ith injection with

$$Y_i = \frac{2(n_{I_2,i} + n_{I_3^-,i})}{n_{H_O^+}} = \frac{\begin{array}{c}2V_{reactor,i}([I_2]_i + [I_3^-]_i \\ -[I_2]_{i-1} - [I_3^-]_{i-1})\end{array}}{V_{injection}[H^+]_O} \tag{13}$$

and

$$Y_{ST,i} = \frac{6[IO_3^-]_{O,i}}{6[IO_3^-]_{O,i} + \left[H_2BO_3^-\right]_{O,i}} \tag{14}$$

where

$$[I_3^-]_i = \frac{D_{O_i}}{\varepsilon_m . L} \tag{15}$$

and

$$V_{reactor,i} = V_{reactor,O} + (i-1) \cdot V_{injection} - (i-1) \cdot V_{sample} \tag{16}$$

$[I_2]_i$ is the solution of the second order equation:

$$-\frac{5}{3}[I_2]_i^2 + \left([I^-]_{O,i} - \frac{8}{3}[I_3^-]_i\right)[I_2]_i - \frac{[I_3^-]_i}{K_B} = 0 \tag{17}$$

The initial concentrations of reactants before each injection must be updated:

$$[I^-]_{O,i} = \frac{\begin{array}{c}(V_{reactor,i-1}[I^-]_{O,i-1}) - \frac{5}{3}(n_{I_2,i-1} + n_{I_{3,i-1}^-}) \\ -n_{I_{3,i-1}^-}\end{array}}{V_{reactor,i-1}} \tag{18}$$

$$[IO_3^-]_{O,i} = \frac{(V_{reactor,i-1}[IO_3^-]_{O,i-1}) - (n_{I_2,i-1} + n_{I_{3,i-1}^-})}{V_{reactor,i-1}} \tag{19}$$

$$[H_2BO_3^-]_{O,i} = \frac{\begin{array}{c}(V_{reactor,i-1}[H_2BO_3^-]_{O,i-1}) \\ -\frac{1}{3}(n_{H_O^+} - 2(n_{I_2,i-1} + n_{I_{3,i-1}^-}))\end{array}}{V_{reactor,i-1}} \tag{20}$$

Another parameter often used to characterise the micromixing efficiency is the micromixedness ratio (α). The micromixedness ratio can be defined as the fraction of perfectly micromixed

volume divided by the fraction of volume remaining segregated [31,35].

$$\alpha = \frac{1 - X_s}{X_s} \tag{21}$$

3. Results and discussion

3.1. Influence of injection time

Before characterising the effect of different parameters, such as stirring speed, and feed location, it has been necessary to quantify the feed time. The injection rate of sulphuric acid should be smaller than the macromixing time scale. For fast sulphuric acid injection conditions, the plume is not well dispersed in the reactor and the results reflect both macro- and mesomixing effects. On the contrary, when injection rate of acid is low, macro- and mesomixing effects are eliminated and the results obtained reflect only micromixing effect [36].

Experimentally, the determination of the critical injection time must be done under worst mixing conditions, at a location far from the impeller and at the lowest stirring speed. In both reactors, four feed times were used for acid injection in feed location P1 (Figs. 1 and 2) and the stirring speed was fixed at 200 rpm, what corresponds to turbulent flow. The results are shown in Fig. 3.

We can see that the segregation index becomes constant for a feed time larger than 140 s for both reactors. These results are in good agreement with those obtained by several authors in stirred batch reactors [14,15,16,22]. For this study, we have fixed the feed time in both reactors higher than this critical feed time, which corresponds to flow rates of about 1 ml/min in the two procedures of injection.

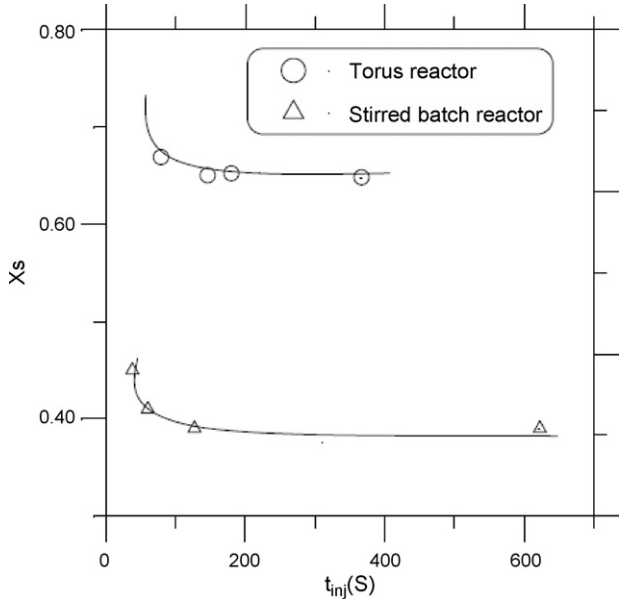

Fig. 3. Effect of feed time on the segregation index in stirred batch and torus reactors.

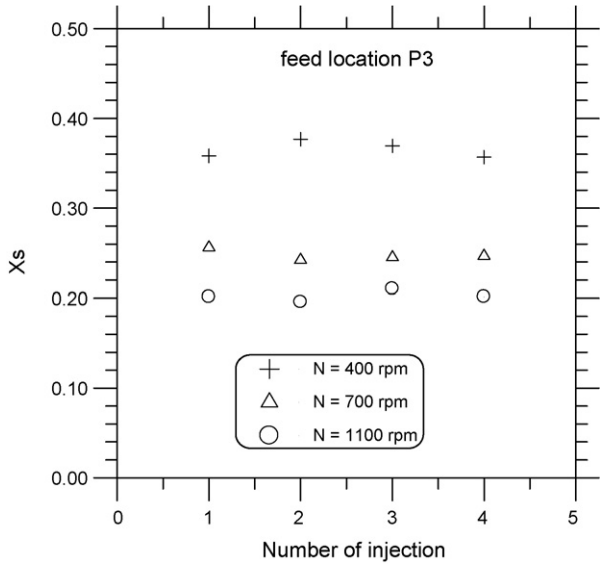

Fig. 4. Comparison of X_s values for successive injections in the torus reactor at feed location P3.

3.2. Method test of successive injections

The experimental procedure of successive injections has been tested in torus rector at feed location P3, for different stirring speeds. For a injection rate of 1 ml/min of sulphuric acid, Fig. 4 shows that, for four successive injections, the segregation index, X_s, is practically constant for the same stirring speed. The results confirm the effectiveness of the successive injection procedure developed by Guichardon and Falk [32] and confirmed, lately, by Assirelli et al. [37].

3.3. Influence of feed location and stirring speed

In batch stirred and torus reactors, three different feed locations (P1, P2, and P3) were studied. The stirring speed was varied within the range from 100 to 1000 rpm and 100 to 1300 rpm, respectively, in the batch stirred and torus reactors. Figs. 1 and 2 show the feed location in the stirred and torus reactors, and the coordinates of these localisations were assembled in Tables 1 and 2.

The effect of stirring speed N on segregation index X_s is shown in Figs. 5 and 6. Firstly, it can be noticed that, for a given feed location, the segregation index decreases similarly in both reactors when the stirring speed increases, and therefore, with increasing mean energy dissipation rate. These results are in good agreement with those cited in the literature, because an increase in stirring speed causes a better micromixing and therefore less selectivity of Dushman reaction (2). On the other hand, the comparison of the evolution of segregation index in both reactors has no practical meaning, because the geometrical characteristics of the two reactors are completely different. The comparison will be carried out later in this paper, using a more relevant criterion.

Secondly, from the same Figs. 5 and 6, we notice that the feed location has an influence on the segregation index. For a given stirring speed, the segregation index decreases similarly in both

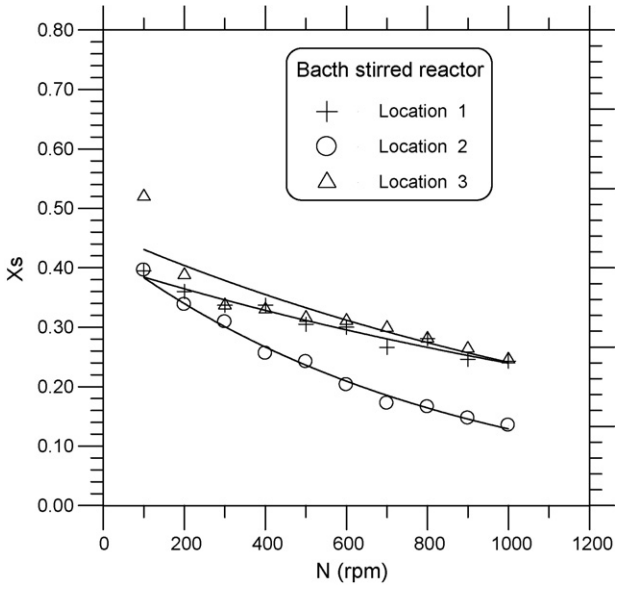

Fig. 5. Effect of stirring speed and feed location on the segregation index in the batch stirred reactor.

reactors when going from a far location to the near location with respect to the impeller, i.e. from locations of low to high local energy dissipation rates, as indicated by LDV studies [38]. To compare the effect of the feed location in torus and stirred batch reactors, it is important to consider the local value of energy dissipation rates in the feed location.

3.4. Comparison of the micromixing efficiency

The local energy dissipation rates can be obtained from the micromixing times by using a simple incorporation model [39] and the turbulence theory of Kolmogorov. In the turbulent flow, the local energy dissipation rates (ε) is proportional to the average energy dissipation rates ($\bar{\varepsilon}$) [36], such as

$$\varepsilon = \phi \cdot \bar{\varepsilon} \tag{22}$$

where ϕ is the proportionality constant, which depends on the position and on the geometry of the reactor.

The mean energy dissipation rate per unit mass is given by the following equation:

$$\bar{\varepsilon} = \frac{N_P \cdot N^3 \cdot d^5}{V} \tag{23}$$

where d is the impeller diameter, N is the stirring speed, N_P is the power number and V is the reaction volume.

In this study, two procedures were used to evaluate the proportionality constant ϕ for both reactors. In the stirred batch reactor, the values of ϕ can be obtained from the literature. For the three feed locations, we have chosen those given by Guichardon [15]. These values (Table 4) were considered to be satisfactory because the micromixing times obtained from these values present a good adequation with the results obtained by the incorporation model [15]. For the six bladed Rushton disc turbine the power number is $N_p = 5.5$ at turbulent flow.

Table 4
Values of ϕ corresponding to the three feed locations in the stirred batch reactor

Positions	ϕ
P1	0.5
P2	4
P3	1

In the case of the torus reactor, the geometry is different and the device of agitation is a marine screw impeller, with $N_p = 0.37$ in turbulent flow. However, another method, based on a numerical computer code, was used in order to calculate the energy dissipation.

3.4.1. Numerical simulation

The distribution of the local energy dissipation rates (ε) in 1 l torus reactor, equipped with marine screw impeller of 36 mm, was carried out with numerical simulation using the commercial code Fluent (Fluent Inc.). This approach has been carried out by Pruvost et al. [40], for the simulation of same torus geometry, using FLUENT software (Fluent Inc.). The first step in the numerical simulation is to create the reactor geometry and to mesh it. The torus shape was three-dimensionally meshed using the Gambit Software (Fluent Inc.) (Fig. 7).

Because of the complex geometry of the marine screw impeller, it is difficult to apply for the entire geometry of the torus reactor a regular mesh. So, the reactor was divided in two distinct zones. The first zone, in the marine screw impeller vicinity has been meshed using tetrahedral volumes and prisms. In the second zone, a regular mesh with elementary hexahedral volumes has been used. The grid discretisation in this regular part is uniform, whereas cell density is gradually increased when coming closer to the impeller.

To mesh the region near the marine screw impeller, a refinement function (named "size function" in Fluent) is applied to control the cells density in boundary layers. This function deter-

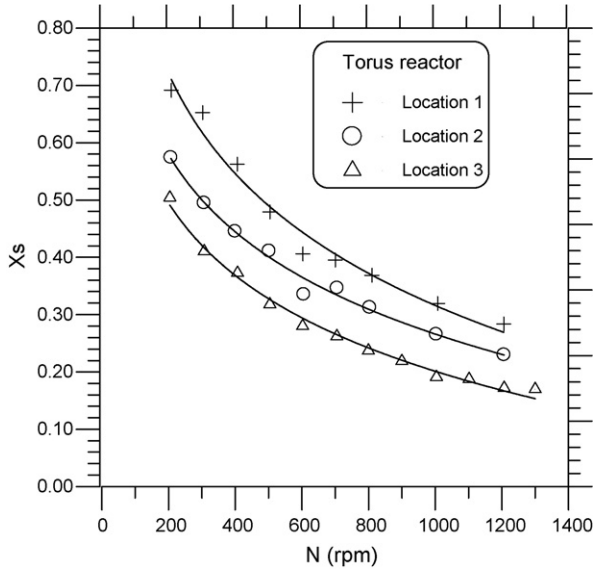

Fig. 6. Effect of stirring speed and feed location on the segregation index in the torus reactor.

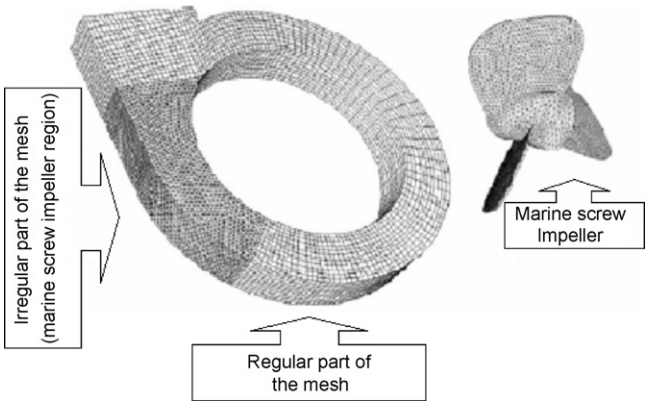

Fig. 7. Mesh topology of the torus reactor.

mines the size of the first near-wall elementary volume and the discretisation step. The resulting grid is composed of 738,896 cells.

The motion of the marine screw impeller was modelled using the multiple reference frames (MRF) resolution, described by Brucato et al. [41] in baffled stirred vessel and utilized by Pruvost et al. [40] in torus geometry.

The flow field was obtained using the k–ω turbulence model [42]. This model was found to give, in the case of torus shape reactor, good results for torus geometry by using the commercial code FLUENT simulation [40,43]. Boundary layers were meshed using a standard wall-function approach, as in Pruvost et al. [43], with an appropriate meshing in the wall region.

The numerical investigation was devoted to characterise the distribution of the values of ϕ, obtained from the local energy dissipation rates (ε) by Eqs. (22) and (23), against the local position (Z_t/L_t) in the reactor (Fig. 8). From this same Fig. 8, we have determined the average values of ϕ corresponding to the various feed locations P1, P2, and P3 used in the torus reactor.

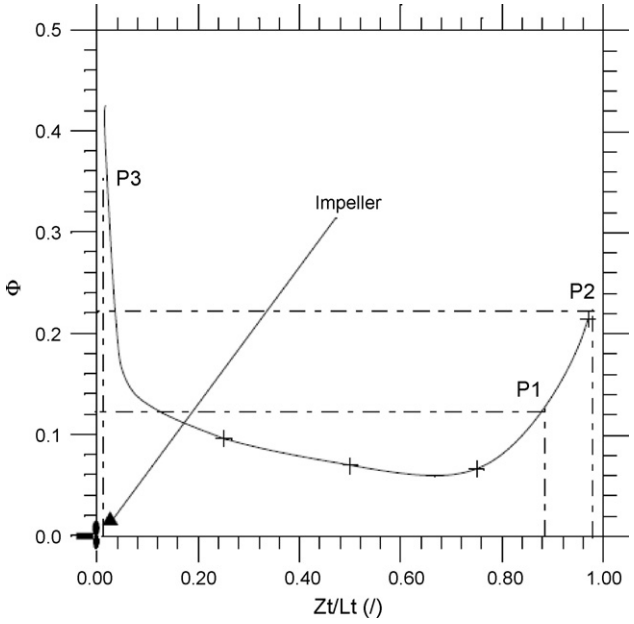

Fig. 8. Distribution of the average values of ϕ, in the torus reactor.

Table 5
Values of ϕ corresponding to the three feed locations in the torus reactor

Positions	ϕ
P1	0.12
P2	0.22
P3	0.35

The results are reported in Table 5. Finally, The local energy dissipation rates, ε, were calculated for different feed locations P1, P2, and P3 using the Eq. (22).

For both reactors and the three feed locations, the micromixedness ratio (α) calculated from Eq. (21) is plotted against local energy dissipation rates, ε (Fig. 9). It can be seen from this figure that, for the torus and the stirred batch reactors the micromixedness ratio is function of local energy dissipation rate and independent on the feed location. These functions are given by the following correlations:

$$\alpha = 5.1\varepsilon^{0.236} \quad \text{torus reactor} \tag{25}$$

$$\alpha = 2.25\varepsilon^{0.183} \quad \text{stirred batch reactor} \tag{26}$$

In the present work, the performance comparison is made by using the micromixing efficiency in both reactors. We note that, for the same value of the local energy dissipation rate, the effectiveness ratio is largely higher in the torus than the stirred batch reactor. This confirms the results obtained by Laederach et al. [44] where they compared the performance of the torus and the stirred batch reactor on the basis of the average energy dissipation. In stirred batch reactors of different volumes, Fournier et al. [31], Falk and Villermaux [45] have found that α is proportional to $\varepsilon^{0.15}$. Then, we note that the exponent corresponding to the different correlations, obtained in batch stirred reactors is approximately constant. However, we can deduce, from these correlations, that the local energy dissipation rate seems not only to be a good criterion for scale-up of micromixing efficiency in

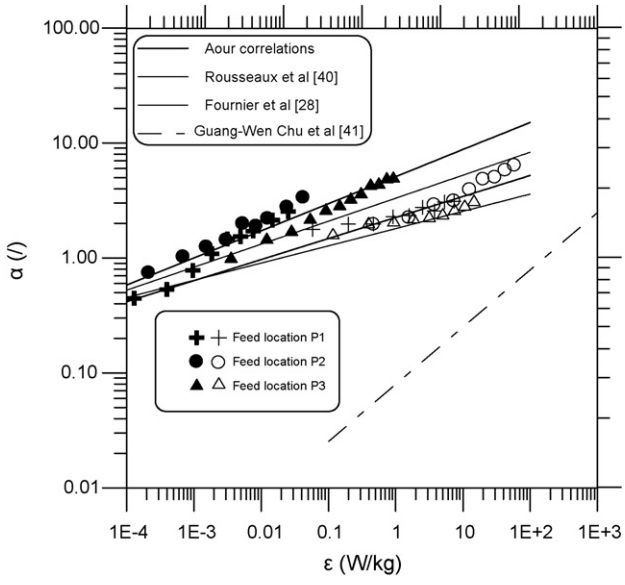

Fig. 9. Effect of the local rate of specific energy dissipation on the micromixedness ratio (α).

the reactors [31,45], but also, a criterion for the comparison of micromixing efficiency, independently of feed location, in different geometries of reactors. Rousseaux et al. [46] and Chu et al. [47] have characterised the micromixing efficiency, respectively, in novel sliding-surface mixing device and a rotor–stator reactor. The local energy dissipation rate was correlated in both devices respectively by $\alpha = 3.3\varepsilon^{0.2}$ and $\alpha = 0.0794\varepsilon^{0.498}$. It can be noticed from Fig. 8 that, for a same value of ε, the micromixedness ratio in the torus reactor remains largely higher than in the sliding-surface mixing device and the rotor–stator reactor.

4. Conclusion

The micromixing efficiency in a torus reactor has been compared with the one of batch stirred reactor. The test reaction system, iodite–iodate, carried out to characterise the effectiveness (α) seems to be reliable and very easy to use. The successive injections procedure is practical, giving reproducible results and is an efficient way of studying micromixing in large volume reactors.

The results obtained for three feed locations in the torus reactor, by using the marine screw impeller, present the same evolution than those obtained in the stirred batch reactor, by using Rushton turbine, i.e. the micromixing efficiency depends of the feed location and stirring speed conditions, and therefore of the mean energy dissipation rate.

The comparison of performance in both reactors, on the basis of local energy dissipation rate (ε), allowed to establish a correlation between effectiveness ration (α) and ε. The results obtained show that $\alpha \propto \varepsilon^{0.236}$ and $\alpha \propto \varepsilon^{0.183}$, respectively, in torus and stirred batch reactor. For a given local energy dissipation rate (ε), we note that the micromixing efficiency in the torus reactor is better than in stirred batch. The comparison of effectiveness ration (α) with other mixing devices shows that the torus reactor is characterised by a high micromixing efficiency.

References

[1] P.V. Danckwerts, The effect of incomplete mixing on homogeneous reactions, Chem. Eng. Sci. 8 (1958) 93–102.

[2] T.N. Zweitering, The degree of mixing in continuous flow systems, Chem. Eng. Sci. 11 (1959) 1–15.

[3] F.L. Paul, J. Mahadevan, J. Foster, M. Kennedy Midler, The effect of mixing on scale up of a parallel reaction system, Chem. Eng. Sci. 47 (1992) 2837–2840.

[4] L. Iris, M. Verschuren, J.G. Wijers, J.T.F. Keurentjes, Effect of mixing on product quality in semibatch stirred tank reactors, AIChE J. 47 (8) (2001) 1731–1739.

[5] B.L. Åslund, Å.C. Rasmuson, Semi-batch reaction crystallization of benzoic acid, AIChE J. 38 (3) (1992) 328–342.

[6] J.Z. Fang, D.J. Lee, Quantitative estimation of segregation indices in CSTR-effects of feed stream and output port, J. Chem. Eng. Jpn. 33 (6) (2000) 923–926.

[7] M. Harada, Micromixing in a continuous flow reactor (coalescence and redispersion models), Mem. Faculty Eng. 24 (1962) 431 (Kyoto University).

[8] J. Villermaux, J.C. Devillon, Représentation de la coalescence et de la redispersion des domaines de ségrégation dans un fluide par modèle d'interaction phénoménologique, in: Proceedings of the 2nd Ind. Symp. Chem. React. Eng., B1, Amsterdam, 1972.

[9] J. Baldyga, J.R. Bourne, Mixing and fast chemical reaction-VIII. Initial deformation of material elements in isotropic homogeneous turbulence, Chem. Eng. Sci. 39 (1984) 329–334.

[10] J. Baldyga, J.R. Bourne, Turbulent mixer model with application to homogeneous, instantaneous chemical reactions, Chem. Eng. Sci. 44 (1989) 1175–1182.

[11] D.Y.C. Ng, D.W.T. Rippin, The effect of incomplete mixing on conversion in homogeneous reaction, Chem. Eng. Sci. 22 (1965) 65.

[12] O. Miyawaki, H. Tsujikawa, Y. Uraguchi, Chemical reactions under incomplete mixing, J. Chem. Eng. Jpn. 8 (1975) 63.

[13] J. Baldyga, J.R. Bourne, The effect of micromixing on parallel reactions, Chem. Eng. Sci. 45 (1990) 907–916.

[14] M.C. Founier, Caractérisation de l'efficacité de micromélange par une nouvelle réaction chimique test, Ph.D. Thesis, INPL Nancy, 1994.

[15] P. Guichardon, Charactérisation chimique du micromélange par la réaction iodure iodate. Ph.D. Thesis, INPL Nancy, 1996.

[16] M. Assirelli, W. Bujalski, A. Eaglesham, A.W. Nienow, Intensifying micromixing in a semi-batch reactor using a Rushton turbine, Chem. Eng. Sci. 60 (2005) 2333–2339.

[17] A. Ducci, M. Yianneskis, Direct determination of energy dissipation in stirred vessels with two-point LDA, AIChE J. 51 (2005) 2133–2149.

[18] M. Micheletti, S. Baldi, S.L. Yeoh, A. Ducci, G. Papadakis, K.C. Lee, M. Yianneskis, On spatial and temporal variations and estimates of energy dissipation in stirred reactors, IChemE 82 (2004) 1188–1198.

[19] S.S. Paul, M.F. Tachie, S.J. Ormiston, Experimental study of turbulent cross-flow in a staggered tube bundle using particle image velocimetry, Int. J. Heat Fluid Flow 28 (2007) 441–453.

[20] J.R. Bourne, R.V. Gholap, An approximate method for predicting the product distribution of fast reactions in stirred tank reactors, Chem. Eng. J. 59 (1995) 293–296.

[21] W.W. Lin, D.J. Lee, Micromixing effects in aerated stirred tank, Chem. Eng. Sci. 52 (1997) 3837–3842.

[22] E. Schaer, P. Guichardon, L. Falk, E. Plasari, Determination of local energy dissipation rates in impinging jets by a chemical reaction method, Chem. Eng. J. 72 (1999) 125–138.

[23] J.Z. Fang, D.J. Lee, Micromixing efficiency in static mixer, Chem. Eng. Sci. 56 (2001) 3797–3802.

[24] E.S. Mickaily-huber, F. Bertrand, P. Tanguy, Numerical simulations of mixing in an SMRX static mixer, Chem. Eng. J. 63 (1996) 117–126.

[25] J.G. Liang, J.F. Chen, J.W. Zhang, Numerical simulation of micromixing in rotating packed bed, Chem. Eng. J. 55 (2004) 882–887.

[26] H.J. Yang, G.W. Chu, Y. Xiang, J.F. Chen, Characterization of micromixing efficiency in rotating packed beds by chemical methods, Chem. Eng. J. 121 (2006) 147–152.

[27] T. Meyer, A. Renken, Characterisation of segregation in tubular polymerisation reactor by a new chemical method, Chem. Eng. Sci. 45 (8) (1990) 2793–2800.

[28] C.I. Liu, D.J. Lee, Micromixing effects in a Couette flow reactor, Chem. Eng. Sci. 54 (1999) 2883–2888.

[29] P. Belleville, L. Nouri, J. Legrand, Mixing characteristics in the torus reactor, Chem. Eng. Technol. 15 (1992) 282–289.

[30] L. Nouri, Ph.D. Etude des performances du réacteur torique-Application à l'hydrolyse enzymatique des protéines végétales, Thesis, Nantes, 1994.

[31] M.C. Fournier, L. Falk, J. Villermaux, A new parallel competing reaction system for assessing micromixing efficiency-determination of micromixing time by a simple mixing model, Chem. Eng. Sci. 51 (23) (1996) 5187–5192.

[32] P. Guichardon, L. Falk, Characterisation of micromixing efficiency by the iodide-iodate reaction system. Part I, Chem. Eng. Sci. 55 (2000) 4233–4243.

[33] P. Guichardon, L. Falk, M. Andrieu, Experimental comparison of the iodide–iodate and the diazo coupling micromixing test reactions in stirred reactors, Chem. Eng. Res. Des. 79 (8) (2001) 906–914.

[34] D.A. Palmer, R.W. Ramette, R.E. Mesmer, Triodide ion formation equilibrium and activity coefficients in aqueous solution, J. Solut. Chem. 13 (9) (1984) 673.

[35] J. Villermaux, Micromixing phenomena in stirred reactors, in: Anon. (Ed.), Encyclopedia of Fluid Mechanics, Gulf Pub, Houston, TX, 1986, pp. 707–771 (Chapter 27).

[36] J. Baldyga, J.R. Bourne, Turbulent Mixing and Chemical Reactions, John Wiley & Sons, Chichester, UK, 1999.
[37] M. Assirelli, W. Bujalski, A. Eaglesham, A.W. Nienow, Study of micromixing in a stirred tank using a Rushton turbine: comparison of feed position and other mixing devices, Trans. Inst. Chem. Eng. A 80 (2002) 855–863.
[38] R. Geisler, R. Krebs, P. Forschner, Local turbulent shear stress in stirred vessels and its significance for different mixing tanks, Chem. Eng. Symp. 136 (1991) 243–250.
[39] J. Baldyga, J.R. Bourne, A fluid mechanical approach to turbulent mixing and chemical reaction, part II. Micromixing in the light of turbulent theory, Chem. Eng. Commun. 28 (1984) 243–258.
[40] J. Pruvost, L. Pottier, J. Legrand, Numerical investigation of hydrodynamic and mixing conditions in a torus photobioreactor, Chem. Eng. Sci. 61 (2006) 4476–4489.
[41] A. Brucato, M. Ciofalo, F. Grisafi, G. Micale, Numerical prediction of flow-fields in baffled stirred vessels: a comparison of alternative modelling approaches, Chem. Eng. Sci. 53 (21) (1998) 3653–3684.
[42] D.C. Wilcox, Turbulence Modelling for CFD, DCW Industries, Inc., La Canada, California, 1998.
[43] J. Pruvost, J. Legrand, P. Legentilhomme, J.M. Rosant, Numerical investigation of bend and torus flows. Part II: low simulation in torus reactor, Chem. Eng. Sci. 59 (2004) 3359–3370.
[44] H. Laederach, F. Widmer, Le bioréacteur torique, Inf. Chim. 249 (1984) 157–160.
[45] L. Falk, J. Villermaux, Numerical scale-up and design of high-efficiency mixers for control and optimisation of the yield and selectivity in chemical reactors, Appl. Therm. Eng. 17 (8–10) (1997) 845–859.
[46] J.M. Rousseaux, L. Falk, H. Muhr, E. Plasari, Micromixing efficiency of a novel sliding-surface mixing device, AIchE J. 45 (1999) 2203–2213.
[47] G.-W. Chu, Y.-H. Song, H.-J. Yang, J.-M. Chen, H. Chen, J.-F. Chen, Micromixing efficiency of a novel rotor–stator reactor, Chem. Eng. J. 128 (2007) 191–196.